GEOLOGY | THE GEOLOGICAL SOCIETY OF AMERICA®

https://doi.org/10.1130/G50138.1

Manuscript received 18 November 2021
Revised manuscript received 15 February 2022
Manuscript accepted 7 May 2022

Published online 18 July 2022

Physical transport of magmatic sulfides promotes copper enrichment in hydrothermal ore fluids

Christoph A. Heinrich and James A.D. Connolly
Department of Earth Sciences, ETH Zürich, Clausiusstrasse 25, 8092 Zurich, Switzerland

ABSTRACT

Loss of magmatic sulfides to the mantle is posited to explain the copper deficit of evolved arc magmas and the depleted Cu/Ag ratio of the continental crust. We address the question of whether saturating sulfides may instead be mechanically entrained with rising magmas, and how this would affect their geochemical fate in the upper crust. Entrainment is plausible considering sulfide wetting properties and settling velocities relative to magma ascent velocities. Entrained sulfide increases the pressure at which magmas become saturated with respect to H-O-S fluids in the upper crust by 10–100 MPa, with the pressure difference increasing with temperature, water content, and oxidation. Bubbles are likely to nucleate on sulfide particles, allowing transfer of S and Cu from the sulfide to the fluid over a small crystallization interval without limitations by diffusion through the silicate melt. This sequence of processes gives magmatic sulfides an active role in ore metal transport and enrichment to form porphyry copper deposits, and may have global implications for crustal Cu budgets.

INTRODUCTION

Porphyry copper deposits contain millions of tons of Cu enriched by orders of magnitude compared to common rocks. These extreme anomalies form by several enrichment steps from magma to fluid to ore (Sillitoe, 2010). The preceding evolution, by contrast, is currently envisioned to be a partial depletion step that is caused by sulfide saturation sequestering chalcophile metals originally present in primary arc basalts (e.g., Chen et al., 2020). A global deficit of Cu in arc volcanics above thick continental crust and in the bulk continental crust (Chiaradia, 2014), combined with common sulfide presence and partial Cu enrichment in lower crustal cumulates (Métrich et al., 1999; Rezeau and Jagoutz, 2020), is believed to indicate significant loss of Cu and other chalcophile metals by recycling to the mantle (Lee et al., 2012; Jenner, 2017; Park et al., 2021). Paradoxically, the Cu deficit of magmatic arc rocks is largest in tectonic settings that also host the world's premier porphyry copper provinces (Chiaradia, 2014; Loucks, 2021). The widespread presence of accessory sulfide in magmas associated with porphyry copper deposits indicates that sulfide saturation in the lower crust is not detrimental to ore formation (Du and Audétat, 2020; Rottier et al., 2020). The suggested roles for magmatic sulfide in the formation of porphyry copper deposits have focused on upper crustal processes; e.g., transient chalcophile element storage, sulfide accumulation and remobilization, bubble-flotation of composite particles, and wholesale or fractional sulfide decomposition upon fluid saturation, which can affect the bulk Au/Cu ratio of resulting ore deposits (Hattori and Keith, 2001; Halter et al., 2004; Nadeau et al., 2010; Wilkinson, 2013; Mungall et al., 2015; Yao and Mungall, 2020). Most recent research has instead focused on identifying tectonic and magmatic conditions that minimize lower crustal Cu loss and optimize chances of making ore deposits from the remaining Cu in evolving magmas (Richards, 2015; Lee and Tang, 2020; Rezeau and Jagoutz, 2020; Chelle-Michou and Rottier, 2021; Park et al., 2021).

We question the prevailing view that sulfide saturation in the lower crust necessarily means sulfide loss and consequent metal depletion of the magma. We explore the alternative possibility that initial enrichment in magmatic sulfide is followed by mechanical entrainment of sulfide particles by ascending silicate melts (Core et al., 2006), and quantify its consequences for magmatic fluid saturation in the upper crust and the transfer of chalcophile metals to this fluid.

PHYSICAL MOBILITY OF MAGMATIC SULFIDES

Experiments measuring dihedral angles between mantle minerals and FeS-rich sulfide melt show that the wetting characteristics of sulfide in contact with silicate grain surfaces favor isolated sulfide spherules in silicate melt (Wang et al., 2020). Grains of monosulfide solid solution commonly forming composite spherules with more Cu- and Ni-rich sulfide melt show no tendency for preferential attachment to major oxides and silicates (e.g., Li and Audétat, 2012).

Whether sulfide particles or droplets settle or remain entrained in the melt is determined by the sinking velocity of sulfide relative to the ascent velocity of the host silicate magma (Tomkins and Mavrogenes, 2003). The density difference between sulfide and silicate melt, $\Delta\rho$, enters linearly into Stokes' formula, whereas particle radius, r, enters by its square for a silicate melt viscosity μ:

$$\text{Sinking velocity } V = 2\,\Delta\rho\,g\,r^2/9\,\mu. \quad (1)$$

Evaluation of Equation 1 (see the Supplemental Material[1]) shows that the dominant compositional effects on viscosity—silica and water content—partly cancel, so that extrapolated curves for basalts approximate more fractionated melts with higher water content at lower temperature (Fig. 1). The size of sulfide

*E-mail: heinrich@erdw.ethz.ch

[1]Supplemental Material. Stokes calculations with assumed model compositions; thermodynamic modeling method with data sources and sensitivity tests; comments on component diffusion in silicate melts; a mass balance estimate for Cu, Ag transfer by entrained sulfide melt; and supplemental references on methods and material properties. Please visit https://doi.org/10.1130/GEOL.S.20044310 to access the supplemental material, and contact editing@geosociety.org with any questions.

CITATION: Heinrich, C.A., and Connolly, J.A.D., 2022, Physical transport of magmatic sulfides promotes copper enrichment in hydrothermal ore fluids: Geology, v. 50, p. 1101–1105, https://doi.org/10.1130/G50138.1

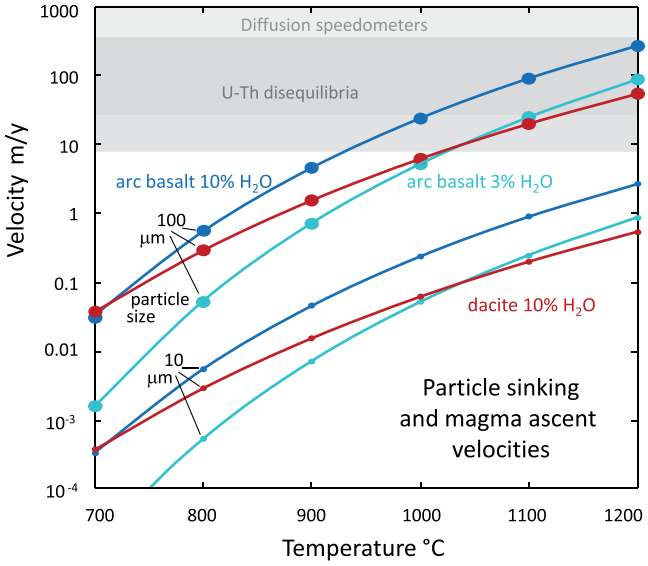

Figure 1. Sinking velocity of sulfide particles in silicate melts as a function of temperature (curves) estimated for three melt compositions (line colors, extrapolated) and two particle sizes (10 μm and 100 μm; indicated by symbol size). Sulfide is entrained if sinking is slower than the ascent velocity of the magma (range shaded in gray).

particles observed as inclusions in magmatic glass and phenocrysts is typically 1–100 μm (Halter et al., 2004; Du and Audétat, 2020; Georgatou and Chiaradia, 2020), and models of sulfide particle growth by diffusion and coalescence indicate an upper limit of ~300 μm (Yao and Mungall, 2020).

Ascent velocities from U-Th series disequilibria are based on transfer duration between the mantle source and the surface that include periods of storage and therefore represent minimum flow velocity (Turner and Costa, 2007). Diffusion-based speedometers yield similar estimates for lower crustal ascent and much faster velocities in the upper crust when fluid saturation initiates volcanic eruptions (Neave and Maclennan, 2020). The comparison (Fig. 1, gray bars) shows that sulfides not removed by inclusion in cumulate crystals may commonly be transported by silicate melts.

THERMODYNAMICS OF SULFIDE DECOMPOSITION DURING VOLATILE SATURATION

Lesne et al. (2015) showed that sulfur dissolved in silicate magmas increases the pressure and depth of magmatic fluid saturation but they did not consider saturation of a separate sulfide phase, which is the focus of our analysis. We explored the relative stability of pyrrhotite, anhydrite, and a H-O-S fluid phase in equilibrium with a variably crystallized magma. The stability and decomposition of Fe-S-rich monosulfide solid solution (simplified to non-stoichiometric FeS) is controlled by reactions linking the partial pressure of gas species to H_2O(m) and FeO(m) in the coexisting silicate melt. At reducing conditions, the dominant S^{-II} species forms as (Mungall et al., 2015):

$$FeS(s) + H_2O(m) = FeO(m) + H_2S(g), \quad (2)$$

and at oxidizing conditions, $S^{+IV}O_2$ forms as:

$$FeS(s) + 3H_2O(m) = FeO(m) + 3H_2(g) + SO_2(g), \quad (3)$$

whereby H_2O(m) controls the dominant fluid species H_2O(g), and O_2 fugacity (f_{O2}) is controlled by $H_2O(g) = 0.5O_2(g) + H_2(g)$. Intermediate-valency S_2(g) and H_2(g) are minor gas species, with the latter limited by $H_2(g) + Fe_2O_3(m)$ 2 FeO(m) + H_2O(m).

We evaluated these reactions by Gibbs energy minimization using the solution models from Holland et al. (2018). Compared to earlier modeling of melt-sulfide-fluid equilibria (cf. Mungall et al., 2015), the amounts of rock-forming minerals in the magma vary simultaneously with the quantities of sulfide and fluid. The model chemistry is simplified compared to that of Yao and Mungall (2020) in that Cl and C are ignored, as is S solubility in the melt (a function of pressure [*P*], temperature [*T*], and melt composition, notably redox conditions; e.g., Matjuschkin et al., 2016). We disregard C because it adds an arbitrary degree of freedom to the model; calculations for plausible melt CO_2 content show that while CO_2 may cause fluid saturation at higher pressure, the quantity of fluid is so small that it has only second-order consequences for de-sulfidation (Fig. S1 in the Supplemental Material). Our approach is simplified but emphasizes the first-order consequence of crystallization for aqueous fluid production as a self-enhancing process because H_2O loss from the melt in turn promotes crystallization. We chose the hydrous arc basalt composition of Rezeau and Jagoutz (2020), similar to that used by Chiaradia (2014) and others, which apply alternative melt models. Amphibole has been excluded because this solution model, implausibly, suppresses magnetite stability, so that pyroxenes take the place of mafic minerals in our model system (see the Supplemental Material). We present results for fixed bulk compositions, rather than cooling paths of fractional crystallization, to illustrate the effects of magmatic sulfide across a *P-T* region (Fig. 2). To introduce S, 0.5 wt% FeS was added to the model basalt composition. The resulting S-content is near the high end of estimates for S in primitive arc basalts compared with S solubility at sulfide saturation (Chelle-Michou and Rottier, 2021) and of petrographic estimates of sulfide abundance in sulfide-saturated mafic arc volcanics (Métrich et al., 1999; Larocque et al., 2000).

At lower crustal conditions, our melt-dominated magma is fluid-free but saturated with pyrrhotite and anhydrite (which, in reality, is partly dissolved in the melt), with mafic minerals, and with + garnet ± feldspar giving way to magnetite-rich spinel + feldspar at mid-crustal pressures. Decompression causes fluid saturation (solid purple curve in Fig. 2B), the pressure of which is increased by the presence of sulfur. The magnitude of this increase, ΔP(S), was obtained by equilibrating the same bulk composition without added FeS (stippled purple curve in Fig. 2B). ΔP(S) increases with increasing temperature, which promotes de-sulfidation by Reactions (2) and (3), so that above ~1000 °C, the fluid saturation curve reverses its slope in the FeS-saturated system (Fig. 2B). With further crystallization, the release of H_2O continues to promote de-sulfidation to the point where all available S is contained in the magmatic fluid phase (dashed lines "Po out," "any out" in Fig. 2B). As a result, total S concentration in the fluid first increases with decreasing pressure but, after exhaustion of S minerals, decreases due to dilution by magmatic H_2O (mol fraction $X_{S,tot} = X_{H2S} + X_{SO2}$ indicated by scales of light to darker orange in Figure 2).

Lowering the bulk Fe^{III}/Fe^{tot} at constant H_2O content leaves the fluid saturation pressure essentially unchanged except at high temperatures (1000 °C), where FeS de-sulfidation is suppressed (Fig. 3A, thick green line) due to the lower stability of SO_2 relative to H_2S (symbol size in Fig. 3B). For the same reason, final pyrrhotite disappearance shifts to lower pressures (Po out; dashed purple versus green lines in Fig. 3A). The SO_2/H_2S ratio in the fluid (Fig. 3B) relates to the redox state of the system as measured by buffer deviations; e.g., $\Delta \log f_{O2}$(QFM) (QFM—quartz-fayalite-magnetite). Varying bulk Fe^{III}/Fe^{tot} from 0.2 to 0.5 increases $\Delta \log f_{O2}$(QFM) from +1.0 to +2.2 (see the Supplemental Material), which is reasonable in light of natural oxybarometers (Richards, 2015; Matjuschkin et al., 2016). Halving the H_2O content from 6 wt% to 3 wt% shifts all curves to lower pressure because fluid saturation requires higher degrees of crystallization.

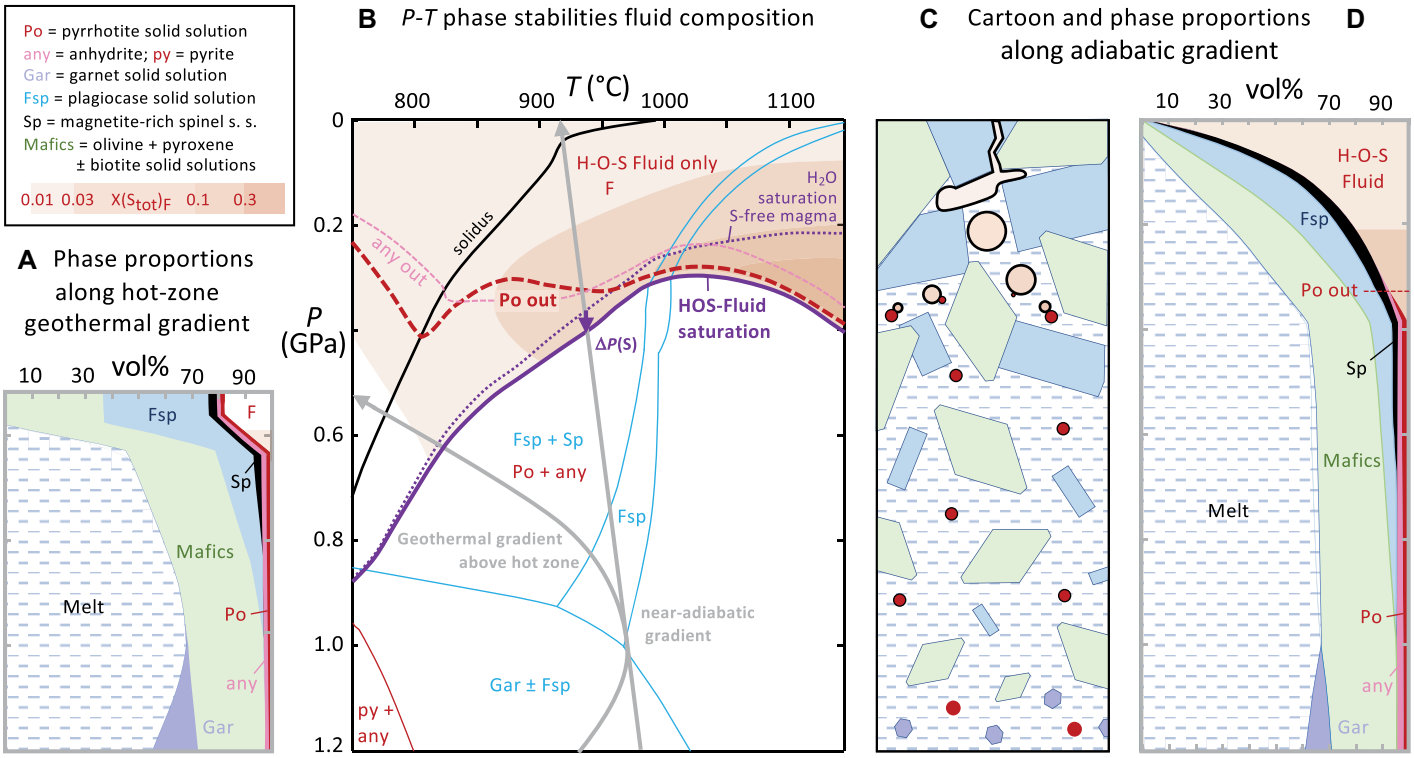

Figure 2. Simplified thermodynamic model for sulfide-saturated hydrous arc basalt. (A) Predicted phase proportions along a hot-zone geothermal gradient. (B) Pressure–temperature (*P-T*) phase diagram section for hydrous (6 wt% H_2O) basaltic magma containing 0.5 wt% pyrrhotite, with phase stability boundaries of S-hosting phases in red to purple colors and main Al-Fe^{III} phases in light blue; mafic minerals and melt coexist at all temperatures above the solidus; two crystallization transects (gray lines) approximate cooling along a geothermal gradient above a magma-rich hot zone in the lower crust (A), or near-adiabatic decompression approximating rapid magma ascent (C,D). Δ*P*(S) is the increase in the fluid (F) saturation pressure due to magmatic S (thick purple line in A) compared to the corresponding S-free model system (stippled line). The cartoon (C) emphasizes the small pressure interval between fluid saturation and sulfide exhaustion ("Po out") due to crystallization-driven fluid generation.

We conclude that sulfides in hot arc magma can persist to the upper crust, where they decompose and transfer S to a hydrous fluid over a small *P-T* interval, well before the magma fully crystallizes (Figs. 2C and 2D). By contrast, along cooler geothermal gradients, the magma reaches fluid saturation at mid-crustal levels; the lower temperature and higher pressure inhibit sulfide decomposition, leading to the dispersal of S-poor aqueous fluid from intrusive rocks that retain their magmatic sulfide phase (Fig. 2A). Both arc-magma cases contrast with volatile-poor, and typically hotter, melt-rich flood basalts, in which minor hydro-carbonic fluid exsolves as a consequence of decompression, with the result that magmatic sulfide persists to near-surface pressures.

BUBBLE SATURATION AND TRANSFER OF ORE-FORMING COMPONENTS

Bubble nucleation in liquids is reduced by mineral surfaces, such that heterogeneous nucleation tends to occur on the mineral with the largest outer angle, Ψ, between mineral and vapor (Fig. 4A). In silicate magmas, typically Ψ is maximized by non-silicate minerals, magnetite, or sulfide (Fiege and Cichy, 2015). Composite fluid + sulfide inclusions in magnetite (Georgatou and Chiaradia, 2020) indicate larger Ψ of vapor against sulfide compared with vapor against magnetite, implying that bubble nucleation is most likely initiated on sulfide particles (Fig. 4A; Wang et al., 2020).

The subsequent growth of a H-O-S–dominated fluid bubble is limited by the diffusion of H_2O through the silicate melt, with H_2O—which is known to diffuse rapidly—being the dominant volatile component in the magma and the reactant driving de-sulfidation (Reactions 2 and 3; Fig. 4B; Zhang and Ni, 2010). By contrast, the transfer of S, Fe, Cu, and other chalcophile metals from a decomposing sulfide particle to an attached fluid bubble requires no diffusive transport through the silicate melt. Therefore, the growing bubble will directly incorporate S and metals from the decomposing sulfide, and bulk metal extraction from magma carrying separate sulfide particles may be faster and more complete than from sulfide-undersaturated magma.

DISCUSSION

If sulfide saturation does not result in sulfide loss, it causes no bulk Cu depletion and is not a limiting factor for ore formation (cf. Chiaradia, 2014; Chelle-Michou and Rottier, 2021). Our results show, to the contrary, that early magmatic sulfide saturation in arc magmas may be a first step in Cu enrichment, actively promoting later porphyry copper ore formation. Optimal conditions for sulfide entrainment and subsequent decomposition to ore-forming fluid match earlier observations of magmas enabling fertile ore provinces, including oxidizing conditions and high water content. Both processes are favored by the rapid ascent of hot, hydrous magmas toward Earth's surface from constrained magma reservoirs fractionating at the base of thickened crust in compressive tectonic settings (Sillitoe, 2010; Loucks, 2021). Our arguments extend the model of Lee and Tang (2020) for porphyry copper ore formation, but little or no Cu needs to be lost at the base of the crust, and no extreme redox conditions due to garnet removal are required.

Physical transport of sulfides and their decomposition upon fluid saturation shifts the focus from chemical modeling of element distribution between sulfide, silicate melt, and fluid (e.g., Chen et al., 2020; Rottier et al., 2020; Chelle-Michou and Rottier, 2021) to the question of surface interaction between sulfide particles (solid or molten) and major minerals that are removed during fractional crystallization

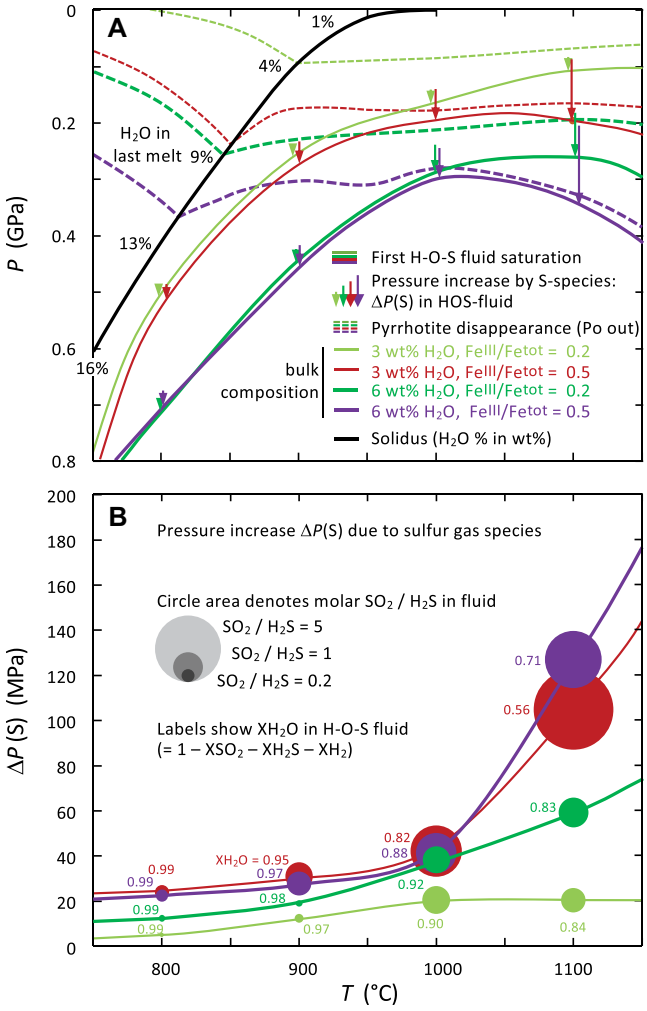

Figure 3. (A) Pressure-temperature (*P-T*) fluid saturation curves for FeS-saturated magma (thick solid lines) and corresponding pyrrhotite stability limits ("Po-out", dashed lines), colored for high and low values of bulk H_2O and Fe^{III}/Fe^{tot} (purple curves correspond to those in Fig. 2B). (B) Increase in fluid saturation pressure due to sulfide entrainment [ΔP(S), arrows in A], compared to the S-free systems, is shown as curves, with symbol sizes indicating the SO_2/H_2S ratio in the fluid.

(Yao and Mungall, 2020). Net S and chalcophile metal depletion would occur by sulfides preferentially attached to major minerals. If sulfides form isolated globules in silicate melt, as available evidence suggests (Wang et al., 2020), the bulk magma may experience net sulfide enrichment so that Cu becomes transiently concentrated like an incompatible element (Cline and Bodnar, 1991) for subsequent transfer to the fluid phase. Such ore metal enrichment can result simply from the entrainment of sulfides with the fractionating silicate melt and does not require prior physical accumulation of sulfides. If re-mobilization of lower-crustal sulfide accumulations indeed adds to further enrichment (Core et al., 2006), as suggested by other researchers (e.g., Chiaradia, 2014; Du and Audétat, 2020), then physical mobilization by rapid magma extraction seems more likely than chemical mobilization, which would require a fundamental magma-chemical change from sulfide precipitation to sulfide re-dissolution. Added buoyancy by sulfide attachment to bubbles and the presence of molten sulfide may enhance enrichment in upper-crustal reservoirs (Mungall et al., 2015), but these conditions are not essential for avoiding metal loss.

The fraction of Cu that can be physically transported to the upper crust depends on sulfide quantity. For 0.2–0.5 wt% FeS and assumed distribution coefficients of Cu or Ag between monosulfide solid solution and silicate melt (400 or 60, respectively; Li and Audétat, 2012), the sulfide phase can carry 45–66% of the initially available Cu to the upper crust (but <20% of initial Ag; see the Supplemental Material). This amount is comparable to the deficit of Cu in volcanic rocks above thick continental crust compared to arc rocks above thin crust (~70%; Chiaradia, 2014) and the Cu/Ag deficit in the bulk continental crust compared to primitive arc basalts (~50%; Chen et al., 2020). Selective depletion of the most chalcophile precious metals (Au, Pd, and Pt) by removal of a small amount of sulfide may explain the giant Cu-only deposits of Chile (Park et al., 2021). However, the low concentration of Pd and Pt in ore deposits is not a conclusive argument against sulfide entrainment and subsequent transfer to magmatic fluid: all these elements are highly soluble at magmatic temperatures (e.g., Sullivan et al., 2022) and their abundance in ore deposits therefore depends on selective precipitation efficiency. Future modeling may combine our approach with partitioning of elements between fluid, sulfide phases, and silicate melt, including dissolved S. Our first-order estimate suggests the possibility that some of the global deficit of chalcophile metals could be due to dispersion via magmatic fluids to the hydrosphere and recycling by sediment subduction (cf. Soyol-Erdene and Huh, 2012) rather than cumulate loss to the mantle alone.

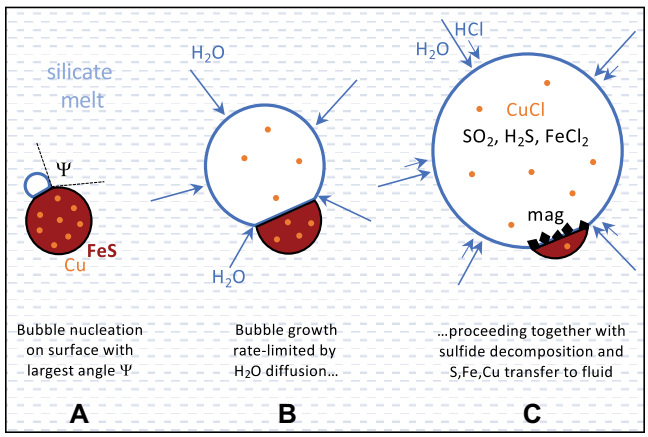

Figure 4. Cartoon showing magmatic fluid generation by direct transfer of ore-forming components (S, Cu, and precious metals including Au, indicated by orange points) from a decomposing sulfide particle (dark red), with partial incorporation of Fe in transient or residual magnetite (mag).

ACKNOWLEDGMENTS

We thank Giada Iacono-Marziano, James Mungall, and Richard Sillitoe for critical reviews that helped clarifying our arguments and we appreciate Marc Norman's thoughtful editorial handling of this paper. Continued support by ETH Zürich and earlier funding by the Swiss National Science Foundation (Project 200020-166151) is acknowledged.

REFERENCES CITED

Chelle-Michou, C., and Rottier, B., 2021, Transcrustal magmatic controls on the size of porphyry Cu systems: State of knowledge and open questions, *in* Sholeh, A., and Wang, R., eds., Tectonomagmatic Influences on Metallogeny and Hydrothermal Ore Deposits: A Tribute to Jeremy P. Richards: Society of Economic Geologists Special Publication 24, p. 87–100, https://doi.org/10.5382/SP.24.06.

Chen, K., Tang, M., Lee, C.T.A., Wang, Z.C., Zou, Z.Q., Hu, Z.C., and Liu, Y.S., 2020, Sulfide-bearing cumulates in deep continental arcs: The missing copper reservoir: Earth and Planetary Science

Letters, v. 531, 115971, https://doi.org/10.1016/j.epsl.2019.115971.
Chiaradia, M., 2014, Copper enrichment in arc magmas controlled by overriding plate thickness: Nature Geoscience, v. 7, p. 43–46, https://doi.org/10.1038/ngeo2028.
Cline, J.S., and Bodnar, R.J., 1991, Can economic porphyry copper mineralization be generated by a typical calc-alkaline melt?: Journal of Geophysical Research: Solid Earth, v. 96, p. 8113–8126, https://doi.org/10.1029/91JB00053.
Core, D.P., Kesler, S.E., and Essene, E.J., 2006, Unusually Cu-rich magmas associated with giant porphyry copper deposits: Evidence from Bingham, Utah: Geology, v. 34, p. 41–44, https://doi.org/10.1130/G21813.1.
Du, J., and Audétat, A., 2020, Early sulfide saturation is not detrimental to porphyry Cu-Au formation: Geology, v. 48, p. 519–524, https://doi.org/10.1130/G47169.1.
Fiege, A., and Cichy, S.B., 2015, Experimental constraints on bubble formation and growth during magma ascent: A review: The American Mineralogist, v. 100, p. 2426–2442, https://doi.org/10.2138/am-2015-5296.
Georgatou, A.A., and Chiaradia, M., 2020, Magmatic sulfides in high-potassium calc-alkaline to shoshonitic and alkaline rocks: Solid Earth, v. 11, p. 1–21, https://doi.org/10.5194/se-11-1-2020.
Halter, W.E., Heinrich, C.A., and Pettke, T., 2004, Laser-ablation ICP-MS analysis of silicate and sulfide melt inclusions in an andesitic complex II: Evidence for magma mixing and magma chamber evolution: Contributions to Mineralogy and Petrology, v. 147, p. 397–412, https://doi.org/10.1007/s00410-004-0563-5.
Hattori, K.H., and Keith, J.D., 2001, Contribution of mafic melt to porphyry copper mineralization: Evidence from Mount Pinatubo, Philippines, and Bingham Canyon, Utah, USA: Mineralium Deposita, v. 36, p. 799–806, https://doi.org/10.1007/s001260100209.
Holland, T.J.B., Green, E.C.R., and Powell, R., 2018, Melting of peridotites through to granites: A simple thermodynamic model in the system KNCFMASHTOCr: Journal of Petrology, v. 59, p. 881–900, https://doi.org/10.1093/petrology/egy048.
Jenner, F.E., 2017, Cumulate causes for the low contents of sulfide-loving elements in the continental crust: Nature Geoscience, v. 10, p. 524–529, https://doi.org/10.1038/ngeo2965.
Larocque, A.C.L., Stimac, J.A., Keith, J.D., and Huminicki, M.A.E., 2000, Evidence for open-system behavior in immiscible Fe-S-O liquids in silicate magmas: Implications for contributions of metals and sulfur to ore-forming fluids: Canadian Mineralogist, v. 38, p. 1233–1249, https://doi.org/10.2113/gscanmin.38.5.1233.
Lee, C.T.A., and Tang, M., 2020, How to make porphyry copper deposits: Earth and Planetary Science Letters, v. 529, https://doi.org/10.1016/j.epsl.2019.115868.
Lee, C.T.A., Luffi, P., Chin, E.J., Bouchet, R., Dasgupta, R., Morton, D.M., Le Roux, V., Yin, Q.Z., and Jin, D., 2012, Copper systematics in arc magmas and implications for crust-mantle differentiation: Science, v. 336, p. 64–68, https://doi.org/10.1126/science.1217313.
Lesne, P., Scaillet, B., and Pichavant, M., 2015, The solubility of sulfur in hydrous basaltic melts: Chemical Geology, v. 418, p. 104–116, https://doi.org/10.1016/j.chemgeo.2015.03.025.
Li, Y., and Audétat, A., 2012, Partitioning of V, Mn, Co, Ni, Cu, Zn, As, Mo, Ag, Sn, Sb, W, Au, Pb, and Bi between sulfide phases and hydrous basanite melt at upper mantle conditions: Earth and Planetary Science Letters, v. 355, p. 327–340, https://doi.org/10.1016/j.epsl.2012.08.008.
Loucks, R.R., 2021, Deep entrapment of buoyant magmas by orogenic tectonic stress: Its role in producing continental crust, adakites, and porphyry copper deposits: Earth-Science Reviews, v. 220, https://doi.org/10.1016/j.earscirev.2021.103744.
Matjuschkin, V., Blundy, J.D., and Brooker, R.A., 2016, The effect of pressure on sulphur speciation in mid- to deep-crustal arc magmas and implications for the formation of porphyry copper deposits: Contributions to Mineralogy and Petrology, v. 171, https://doi.org/10.1007/s00410-016-1274-4.
Métrich, N., Schiano, P., Clocchiatti, R., and Maury, R.C., 1999, Transfer of sulfur in subduction settings: An example from Batan Island (Luzon volcanic arc, Philippines): Earth and Planetary Science Letters, v. 167, p. 1–14, https://doi.org/10.1016/S0012-821X(99)00009-6.
Mungall, J.E., Brenan, J.M., Godel, B., Barnes, S.J., and Gaillard, F., 2015, Transport of metals and sulphur in magmas by flotation of sulphide melt on vapour bubbles: Nature Geoscience, v. 8, p. 216–219, https://doi.org/10.1038/ngeo2373.
Nadeau, O., Williams-Jones, A.E., and Stix, J., 2010, Sulphide magma as a source of metals in arc-related magmatic hydrothermal ore fluids: Nature Geoscience, v. 3, p. 501–505, https://doi.org/10.1038/ngeo899.
Neave, D.A., and Maclennan, J., 2020, Clinopyroxene dissolution records rapid magma ascent: Frontiers of Earth Science, v. 8, https://doi.org/10.3389/feart.2020.00188.
Park, J.W., Campbell, I.H., Chiaradia, M., Hao, H., and Lee, C.T., 2021, Crustal magmatic controls on the formation of porphyry copper deposits: Nature Reviews Earth & Environment, v. 2, p. 542–557, https://doi.org/10.1038/s43017-021-00182-8.
Rezeau, H., and Jagoutz, O., 2020, The importance of H_2O in arc magmas for the formation of porphyry Cu deposits: Ore Geology Reviews, v. 126, https://doi.org/10.1016/j.oregeorev.2020.103744.
Richards, J.P., 2015, The oxidation state, and sulfur and Cu contents of arc magmas: Implications for metallogeny: Lithos, v. 233, p. 27–45, https://doi.org/10.1016/j.lithos.2014.12.011.
Rottier, B., Audétat, A., Koděra, P., and Lexa, J., 2020, Magmatic evolution of the mineralized Stiavnica volcano (Central Slovakia): Evidence from thermobarometry, melt inclusions, and sulfide inclusions: Journal of Volcanology and Geothermal Research, v. 401, https://doi.org/10.1016/j.jvolgeores.2020.106967.
Sillitoe, R.H., 2010, Porphyry copper systems: Economic Geology, v. 105, p. 3–41, https://doi.org/10.2113/gsecongeo.105.1.3.
Soyol-Erdene, T.O., and Huh, Y., 2012, Dissolved platinum in major rivers of East Asia: Implications for the oceanic budget: Geochemistry Geophysics Geosystems, v. 13, https://doi.org/10.1029/2012GC004102.
Sullivan, N.A., Zajacz, Z., Brenan, J.M., and Tsay, A., 2022, The solubility of platinum in magmatic brines: Insights into the mobility of PGE in ore-forming environments: Geochimica et Cosmochimica Acta, v. 316, p. 253–272, https://doi.org/10.1016/j.gca.2021.09.014.
Tomkins, A.G., and Mavrogenes, J.A., 2003, Generation of metal-rich felsic magmas during crustal anatexis: Geology, v. 31, p. 765–768, https://doi.org/10.1130/G19499.1.
Turner, S., and Costa, F., 2007, Measuring timescales of magmatic evolution: Elements, v. 3, p. 267–272, https://doi.org/10.2113/gselements.3.4.267.
Wang, Z.J., Jin, Z.M., Mungall, J.E., and Xiao, X.H., 2020, Transport of coexisting Ni-Cu sulfide liquid and silicate melt in partially molten peridotite: Earth and Planetary Science Letters, v. 536, https://doi.org/10.1016/j.epsl.2020.116162.
Wilkinson, J.J., 2013, Triggers for the formation of porphyry ore deposits in magmatic arcs: Nature Geoscience, v. 6, p. 917–925, https://doi.org/10.1038/ngeo1940.
Yao, Z.S., and Mungall, J.E., 2020, Flotation mechanism of sulphide melt on vapour bubbles in partially molten magmatic systems: Earth and Planetary Science Letters, v. 542, p. 1–14, https://doi.org/10.1016/j.epsl.2020.116298.
Zhang, Y.X., and Ni, H.W., 2010, Diffusion of H, C, and O Components in Silicate Melts, *in* Zhang, Y.X., and Cherniak, D.J., eds., Diffusion in Minerals and Melts: Reviews in Mineralogy & Geochemistry, v. 72, p. 171–226, https://doi.org/10.1515/9781501508394-006.

Printed in USA